

## Physiological and Ultrastructural Responses of *Nostoc* sp. (*Cyanobacteriota*) Strains to Phosphorus Starvation under Non-Diazotrophic Conditions

P. N. Scherbakov<sup>a, \*</sup>, I. O. Selyakh<sup>a</sup>, L. R. Semenova<sup>a</sup>, O. B. Chivkunova<sup>a</sup>, O. I. Baulina<sup>a</sup>, O. V. Karpova<sup>a</sup>, E. S. Lobakova<sup>a</sup>, A. E. Solovchenko<sup>a</sup>, and O. A. Gorelova<sup>a</sup>

<sup>a</sup> Faculty of Biology, Moscow State University, Moscow, 199234 Russia

\*e-mail: 06keeper60@gmail.com

Received March 5, 2024; revised May 27, 2024; accepted May 27, 2024

**Abstract**—Phosphorus (P) is an essential macronutrient central to the exchange and storage of energy and information in the cell. Due to its limited bioavailability, P often becomes a limiting nutrient in aquatic and terrestrial ecosystems hence the studies of responses to stress caused by P starvation cyanobacteria, the primary producers, are of considerable interest. Indeed, the availability of P is among main factors limiting diazotrophy in cyanobacteria. To gain a deeper understanding of the effect of P starvation on cyanobacteria in non-diazotrophic conditions, we studied a model system of two near—isogenic strains, *Nostoc* sp. PCC 7120 and *Nostoc* sp. PCC 7118 differ in their ability to form heterocysts. Specifically, we investigated the differences in the responses of these strains to P starvation by comparing their growth kinetics, photosynthetic pigment content, ultrastructural rearrangements of vegetative cells, and the expression profile of key genes of phosphorus metabolism. The tolerance of PCC 7120 to P starvation was higher than that of PCC 7118, which manifested itself in a higher growth rate, less profound ultrastructural changes (in particular, phycobilisomes as well as polyphosphate reserves were retained in the cells of PCC 7120). At the same time, the accumulation of cyanophycin, a depot of nitrogen and energy, increased several-fold in the cells of both strains during P starvation, but this increase was larger in PCC 7118 cells. Assumably, the increased resilience of the PCC 7120 to P starvation stems from its higher ability to accumulate intracellular reserves of P in the form of polyphosphates. Our findings suggest that the phenotypic differences between the strains *Nostoc* sp. PCC 7118 and *Nostoc* sp. PCC 7120 are not limited to the different ability to form heterocysts. A deeper understanding of the drivers of stress response phenotypic diversity in near-isogenic strains would require a comparative analysis of their whole-genome sequences.

**Keywords:** cyanobacteria, phosphorus starvation, ultrastructure, cyanophycin, diazotrophy

**DOI:** 10.1134/S0026261724605359

Phosphorus (P) is a key macronutrient integral to nucleic acids, phospholipids, phosphorylated proteins and other phosphometabolites; it is central to the storage and exchange of energy and information in the cell (Blank, 2012). The main bioavailable species of P is inorganic phosphate ( $P_i$ ), which is taken up by the cells of microorganisms, including cyanobacteria, mainly in the form of a single-charge orthophosphate anion. Although P is quite common in the Earth crust, ranking 11th in abundance, photoautotrophic organisms normally experience a shortage of bioavailable P (Gross, 2017; Daneshgar et al., 2018). One of the reasons of scarce bioavailability of P is its high reactivity; because of it, P exists mainly in the form of poorly soluble compounds (Bennett and Elser, 2011). At the same time, P slowly enters the biosphere, mainly during the weathering of P-containing rocks (Gross, 2017). As a result, P becomes a limiting macronutrient

in aquatic and terrestrial ecosystems even more often than nitrogen or sulfur (Cordell and White, 2014; Chen and Graedel, 2016).

During evolution, both cyanobacteria and microalgae have developed a complex response to the stress caused by low availability of P in the environment (Grossman and Aksoy, 2015). This response includes several mechanisms implemented with participation of genes transcriptionally regulated in response to intracellular level of  $P_i$  (Dyhrman, 2016). The mechanisms of “cellular economy” of P include the mobilization of P reserves, primarily polyphosphates, PolyP (Kulaev et al., 2004; Sanz-Luque et al., 2020) and salvaging of P-rich metabolites and cell components (e.g. ribosomal RNA) accumulated in excess during the period of high availability of P. Phospholipids are also replaced by betaine lipids and sulfolipids with similar physical-chemical properties

(Canavate et al., 2017; Muhlroth et al., 2017). Shortage of the mineral nutrients, including P, declines the expression of genes encoding components and enzymes responsible for CO<sub>2</sub> fixation, protein biosynthesis, as well as structural components of the photosynthetic apparatus (PSA)—photosystem proteins, phycobiliproteins of the light-harvesting antenna, and the electron carriers (Ludwig and Bryant, 2012; Teikari et al., 2015). A slowdown of central metabolism shrinks the metabolic sink for photoassimilates triggering a reduction of PSA and the accumulation of carbon reserves in the cell (Collier and Grossman, 1992). Energy-intensive processes such as fixation of atmospheric nitrogen by diazotrophic cyanobacteria species are also inhibited by the nutrient shortage (Raven, 2008).

The above-mentioned processes lead to changes in the morphology and ultrastructure of the cell—the phenotypic hallmarks of the operation of the molecular mechanisms of P starvation responses. Notably, most of the reports on the ultrastructure of cyanobacteria present the results of short-term experiments lasting from several hours (Stevens et al., 1981) to several days (Jensen and Sicko, 1974) though certain experiments lasted from 11 (Solovchenko et al., 2020) to 20 days (Barlow et al., 1979). Thus, it is important to study the long-term effects of P starvation in cyanobacteria, especially on the background of high nitrogen availability. This approach is also practically relevant since cyanobacteria are frequently employed for biomass growing in and biotreatment of P-depleted wastewater (Nesbitt, 1966; Jämsä et al., 2017).

In this work, two closely related strains of cyanobacteria genus *Nostoc* were studied: *Nostoc* sp. PCC 7118 (hereinafter referred to as PCC 7118) and *Nostoc* sp. PCC 7120 (referred to below as PCC 7120). PCC 7118 is a short-chain heterocystless near-isogenic strain that is known to fix nitrogen when deprived of combined nitrogen under anaerobic conditions (Sato and Wada, 1996; Elhai and Wolk, 1990; Sato et al., 2012). The lack of P in the environment is a stressor for both organisms. The aim of this work was to compare the morphophysiological reorganization of these strains under conditions of P starvation and high nitrogen availability preventing heterocyst formation.

## MATERIALS AND METHODS

**The objects** of the study were the strains of filamentous cyanobacteria *Nostoc* sp. PCC 7120 (diazotrophic strain) and PCC 7118 (incapable of aerobic diazotrophy) obtained from the Pasteur Collection of Cyanobacteria, PCC (Paris, France). The pre-cultures of the studied strains were grown under aerobic conditions in 0.75-L Erlenmeyer flasks with 300 mL of BG-11 medium (Stanier et al., 1971) at 25°C and constant illumination (40 μmol PAR quanta m<sup>-2</sup> s<sup>-1</sup>) in and Innova 44R incubator shaker (New Brunswick, Fram-

ingham, Massachusetts, Unites States). Experimental cultivation was carried out as described earlier (Solovchenko et al., 2020) in glass columns (0.6 L, i.d. 4 cm). To induce P starvation, the cells of the preculture were harvested by centrifugation (1500 g, 7 min), washed twice with a P-free BG-11 medium (referred to below as BG-11-P) where KH<sub>2</sub>PO<sub>4</sub> was replaced with K<sub>2</sub>SO<sub>4</sub>, resuspended in BG-11-P medium, and incubated under the conditions described above.

**The dry biomass content** was determined gravimetrically: the cells were deposited on pre-dried and pre-weighed (1801MP8 balances, Sartorius GmbH, Göttingen, Germany) nitrocellulose filters 24 mm in diameter and pore size 0.22 μm (Merck-Millipore, Billerica, Massachusetts, Unites States). The filters with the cells deposited on them were oven dried to a constant weight at 105°C and weighed.

**The optical density (OD) spectra** of cyanobacteria cell suspensions were recorded using a Cary 300 spectrophotometer (Agilent, Santa Clara, California, Unites States) equipped with an integrating sphere from the same manufacturer. The spectra were corrected for the effect of light scattering (Merzlyak and Naqvi, 2000). OD in the band of the long-wavelength maximum of chlorophyll *a* was used as a proxy for chlorophyll *a* content; for assessment of the phycobilin content, the OD ratio OD<sub>624</sub>/OD<sub>678</sub> was used (Parshina et al., 2024; Zlenko et al., 2024).

**Light microscopy.** Bright-field images of the cyanobacterial cell suspensions were obtained using a Leica DM2500 microscope equipped with a Leica DFC 7000T digital camera (Leica Microsystems GmbH, Wetzlar, Germany).

**Electron microscopy.** The ultrastructure of the cyanobacterial cells was studied using transmission electron microscopy (TEM) of ultrathin (<70 nm) sections. The cells were fixed according to a previously published protocol (Gorelova et al., 2015) sequentially in a 2% solution of glutaraldehyde in 0.1 M cacodylate buffer and in 1% (wt/vol) solution of OsO<sub>4</sub> in the same buffer. After dehydration, the samples were embedded in Araldite epoxy resin (Sigma-Aldrich, Saint-Louis, Missouri, Unites States), the ultrathin sections were obtained on a Leica EM UC7 ultramicrotome (Leica Microsystems, Vienna, Austria). Ultrathin sections were stained with lead citrate (Reynolds, 1963) and examined with a JEM-1011 or JEM-1400-Flash electron microscope (JEOL, Tokyo, Japan).

**Morphometry** of vegetative cells was performed on centrally longitudinal sections of trichomes encompassing terminal or intercalary cells with one or two well-resolved adjacent septa, respectively. Only random sections were included into analysis; a series of sections were excluded from the measurements. The number of subcellular structures and inclusions was calculated. The frequency of detection (occurrence) of structures and inclusions was calculated as the proportion of cell sections containing the object of interest

**Table 1.** The qRT-PCR primers used in this work

Target gene (ID)	Designation	Sequence
Pyrophosphatase, <i>ppa</i> (all3570*)	ppaRT fwd	GCTACGCTCACGTA AAAATCTTTG
	ppaRT rev	TTTGTA ACTACGGAAAACTCAGC
Polyphosphate kinase 1, <i>ppk1</i> (alr3593)	ppk1RT fwd	TCGTCTATGGTTTAGTGGGTCT
	ppk1RT rev	CTGTATAGAGTCGTGCCGTTT
Polyphosphate kinase 2, <i>ppk2</i> (all2088)	ppk2RT fwd	GTAAATGATGTGCGTGAAAGGG
	ppk2RT rev	GTGTAAACCATTTGCGATCGG
Exopolyphosphatase, <i>ppx</i> (all3552)	ppxRT fwd	GAGAATGACAAATGCCGAAAGAG
	ppxRT rev	AATGACTCCACACCCAACAG
Polyphosphate glucokinase, <i>ppgk</i> (all1371)	ppgkRT fwd	AAAGGTAAGGGTGTAGAGTTGG
	ppgkRT rev	CTTCGTAAGTTTCCCCTTTGC
$P_i$ -transporter, <i>pstS1</i> (all4575)	pstS1RT fwd	ACTAGCTTACA ACTTGCCCTGG
	pstS1RT rev	AGGTTGACATTAGGGTTAGCAG
$P_i$ -transporter, <i>pstS2</i> (all0911)	pstS2RT fwd	GATGACGGATGCTGAAATTGC
	pstS2RT rev	TGTTGCACGGGATAATCTGAG
Ribonuclease A, <i>rnpA</i> (alr3413)	rnpART fwd	GCGAGCATTAAAACCGTCATC
	rnpART rev	ACCGCCCTCTTACTA ACTTTG

\* According to CyanoBase (<https://genome.microbedb.jp>).

from the total number of analyzed cell sections. The linear dimensions, as well as the area of subcellular structures, were measured on the TEM micrographs of ultrathin cell sections ( $n \geq 25$ ) using the Fiji (Image J) v. 20200708-1553 software (NIH, Bethesda, Massachusetts, Unites States).

Ultrastructural reorganization of the cyanobacterial cells was quantified via changes in the protoplast area and the occurrence (frequency of detection on non-serial sections), the total area, and abundance (number per cell section) of carboxysomes (C), polyphosphate granules (PolyP), cyanophycin granules (CG), poly- $\beta$ -hydroxybutyrate (Phb), and lipid  $\beta$ -granules ( $\beta$ -granules), as well as changes in phycobilisome height and width. In addition, the abundance of ribosomes, the size of nucleoid zones, the abundance and extent of thylakoids were visually assessed. During quantitative morphometry of PolyP, only granules  $>25$  nm in diameter were counted.

**Real-time PCR.** Total RNA was isolated from the cells (approx. 100 mg, fresh weight) pelleted by centrifugation (1500 g, 7 min) and ground in a FastPrep-24 5G homogenizer (MP BioMedicals, Unites States) using a GeneJET RNA purification kit (Thermo Fisher Scientific, Unites States). cDNA synthesis was performed using the Maxima 1st strand cDNA reverse transcription kit (Thermo Fisher Scientific, Unites States). Real-time PCR (qRT-PCR) was performed using the QuantiTect SYBR Green PCR kit (Qiagen, Unites States) on a QuantStudio 7 Flex amplifier (Applied Biosystems, Unites States). The primers for PCR amplification of the target genes (Table 1) were designed using the Real Time PCR Tool (Integrated

DNA Technologies, Unites States). The raw data were processed in the Thermo Fisher Cloud online application for qRT-PCR. The number of specific transcripts in qRT-PCR was determined relative to the amount of the *rnpA* ribonuclease transcript (the endogenous control). The change in the expression level was calculated relative to the expression level in logarithmic culture cells on a complete BG-11 medium. The qRT-PCR tests were performed in two biological replications with two analytical replicas for each.

**Statistical treatment.** All experiments except qRT-PCR (see above) were carried out in three biological replications with two analytical replicas for each. Averages together with their corresponding standard errors are shown in the figures unless stated otherwise. Significance of differences between the average values was tested with ANOVA in Excel spreadsheet software (Microsoft, Redmond, Washington, Unites States).

## RESULTS

**The kinetics of the biomass, chlorophyll, and phycobilin contents.** The studied strains exhibited close growth rates both in complete BG-11 and P-free BG-11–P media during the first 8 days, but the maximum biomass content on 8th day achieved in the complete media was approximately 16% higher than in the absence of P (Fig. 1). In the complete medium, both strains synchronously reached the stationary growth phase by 12th day of cultivation. The accumulation of biomass in the P-free medium stopped by day 8 (in PCC 7118) or later (by day 11–12 in PCC 7120). Later, approximately twofold decrease in biomass content

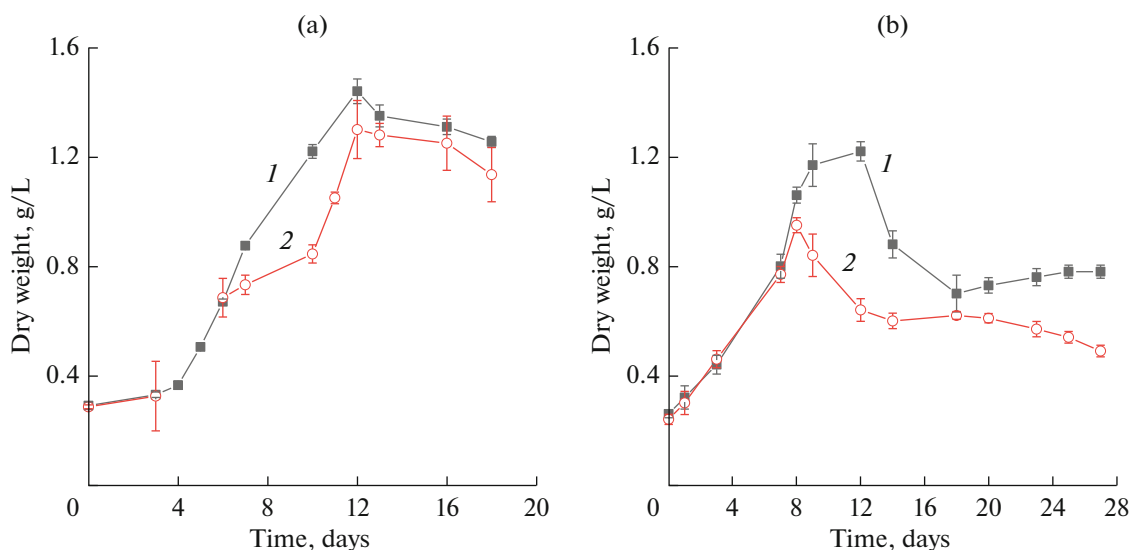


**Fig. 1.** Changes in biomass accumulation by *Nostoc* sp. PCC 7120 (1) and *Nostoc* sp. PCC 7118 (2) cultures grown in (a) complete or (b) P-free medium.

was observed which was more pronounced in PCC 7118 after the 18th day. The PCC 7118 strain showed a further reduction in the biomass content, in contrast to the PCC 7120 culture. Notably, upon replacement of the P-free medium with complete BG-11 medium after 28 days of P starvation the PCC 7120 culture resumed growth, which was not the case in PCC 7118 (data not shown).

For additional assessment of the physiological condition of the cultures, their photosynthetic pigment (chlorophyll *a* and phycobilin) content was followed by monitoring their optical density in the corresponding spectral ranges (see Methods). In the complete medium, the kinetics of chlorophyll *a* content generally corresponded to the kinetics of biomass accumulation, while PCC 7118 accumulated chlorophyll more slowly in the logarithmic growth phase than PCC 7120 (Fig. 2a). Both strains demonstrated an increase in the content of chlorophyll *a* during the initial period of cultivation in the absence of P (Fig. 2b). This increase was more pronounced in PCC 7118 for the first 7–8 days. Later, chlorophyll *a* content declined; this decline was sharper in PCC 7118 (Fig. 2b).

The trends of change in relative phycobilin content during P starvation in PCC 7120 and PCC 7118 differed significantly (Fig. 2c). Thus, in PCC 7120 cultures, a retention or even a slight increase in phycobilins relative to chlorophyll *a* was observed. Likely, this indicates a synchronous reduction of the PSA, which was confirmed with the TEM of cell sections (see below). PCC 7118 was characterized by a dramatic drop in this parameter (Fig. 2c). Sustainable loss of phycobilins was recorded along with a sharp decrease in chlorophyll *a*, which occurred during 8–10 days of

P starvation and continued during the rest 10–27 days when the chlorophyll concentration was already low (Figs. 2b, 2c).

**Morphology of the trichomes and cells.** The availability of  $P_i$  in the medium exerted a significant strain-specific effect on the morphology of the trichomes and vegetative cells. The cyanobacteria cultivated in the P-sufficient medium displayed a morphology typical of the taxon they belong to. They were constituted by oval or barrel-shaped cells formed chains lacking sheath discernible on the bright-field images but possessing clearly distinguishable constrictions in the septal zones; the cells were evenly distributed along the trichome dividing by a symmetrical binary division in a plane perpendicular to the axis of the trichome (Figs. 3a, 3c). PCC 7118 trichomes contained from 2–4 to 25–40 cells which were 3.54–6.68  $\mu\text{m}$  long ( $5.22 \pm 0.8 \mu\text{m}$  on an average) and 4.0–5.9  $\mu\text{m}$  wide ( $5.04 \pm 0.53 \mu\text{m}$  on an average). PCC 7120 trichomes were larger containing from several dozen to 150 cells which were 3.63–7.95  $\mu\text{m}$  long ( $6.03 \pm 1.1 \mu\text{m}$ ) and 4.33–6.8  $\mu\text{m}$  wide ( $5.25 \pm 0.62 \mu\text{m}$  on an average).

During P starvation of PCC 7118 its cells faded, the longer trichomes shortened, and the shorter trichomes died. Thus, the 11 day-old P-deprived culture was dominated by trichomes of 8–18 completely or partially bleached cells (Fig. 3b) which were  $4.97 \pm 0.55 \mu\text{m}$  long and  $5.41 \pm 0.34 \mu\text{m}$  wide. Dividing cells were detected in the shortened trichomes, and the daughter cells were equal or unequal in size.

The signs of P starvation stress were also noted in the PCC 7120 cultures of the same age. Although the length of the trichomes was generally retained, their morphology changed: apart from blue-green cells, a

yellow-green color became noticeable and less uniform (Fig. 3d). The average cell sizes decreased to  $4.93 \pm 0.98$  and  $5.04 \pm 0.53$   $\mu\text{m}$  (length and width, respectively). Cell groups  $10.47 \pm 0.14$   $\mu\text{m}$  long and  $5.74 \pm 0.5$   $\mu\text{m}$  wide located one after another and flanked by deeper constrictions were noted in the trichomes. Such groups frequently included 4 disc-shaped cells which were  $2.8 \pm 0.48$   $\mu\text{m}$  long and  $5.28 \pm 0.5$   $\mu\text{m}$  wide. The P-starving cultures also displayed accelerated cytotomy when the daughter cells did not reach the size of the mother cells is a manifestation of early stress response exercised by the trichome as an individual. There were also abnormally dividing cells whose division plane was not perpendicular but parallel to the trichome longitudinal axis (Fig. 3d).

**Ultrastructure of vegetative cells.** The ultrastructure of vegetative cells of both strains grown in complete BG-11 medium until the stationary phase was typical of the sheath-less representatives of the genus *Nostoc* (Figs. 4a, 4b, 4e, 4f). The ultrathin section micrographs of these cells revealed the gram-negative type of cell wall. The bulk of the protoplast was occupied by thylakoids with a narrow lumen. Groups of 3–6 collinear thylakoids, bent in different directions, were distributed over the entire area of the protoplast. The thylakoid groups surrounded the nucleoid zones harboring compactly arranged DNA strands and peripheral clusters of ribosomes. On their cytoplasmic surface, the thylakoids carried phycobilisomes. Carboxysomes (polyhedral bodies) containing ribulose biphosphate carboxylase/oxygenase (RuBisCO) as the main component were confined to the nucleoid zones.

Reserve compounds in the form of glycogen ( $\alpha$ -granules), lipids ( $\beta$ -granules), and cyanophycin (a copolymer of arginine and aspartic acid) granules (CG) as well as poly- $\beta$ -hydroxybutyrate (Phb) were not abundant but were detected regularly on the cell sections. On the periphery of the Phb, in the nucleoid zones, and in the inter-thylakoid space, electron-dense inclusions were detected. These inclusions were previously shown with EDX spectroscopy to be P-containing reserves mainly in form of PolyP (Ismagulova et al., 2018; Solovchenko et al., 2020).

Earlier we proposed the cessation of cell division and accumulation of dry biomass of the culture as a reliable criterion of the onset of P starvation (Solovchenko et al., 2020). In PCC 7118, this took place on the 8th day of P starvation, and in PCC 7120—on the 12th day of P starvation. We investigated the ultrastructural rearrangements of the cyanobacterial cells at advanced stages of P starvation but before the onset of irreversible changes which was, according to our previous estimations, around 18 days of incubation without P for PCC 7118 and 27 days for PCC 7120 (Figs. 4c, 4d, 4g, 4h).

The most spectacular rearrangements affected the internal organization of protoplasts and were similar in

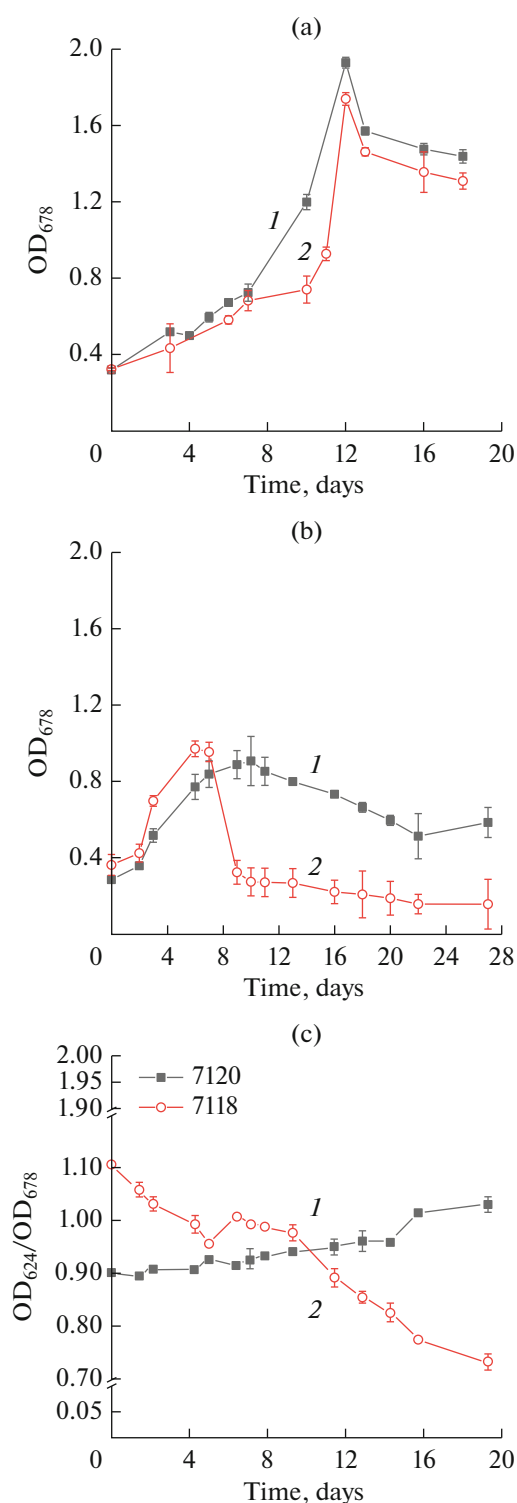


**Fig. 2.** Changes of the OD in the long-wave absorption maximum of chlorophyll *a*, OD<sub>678</sub> (a, b) and the ratio of OD<sub>624</sub> (phycobilin absorption band) to OD<sub>678</sub> (c) in *Nostoc* sp. PCC 7120 (1) and *Nostoc* sp. PCC 7118 (2) cultures incubated (a) in complete or (b, c) P-free medium.

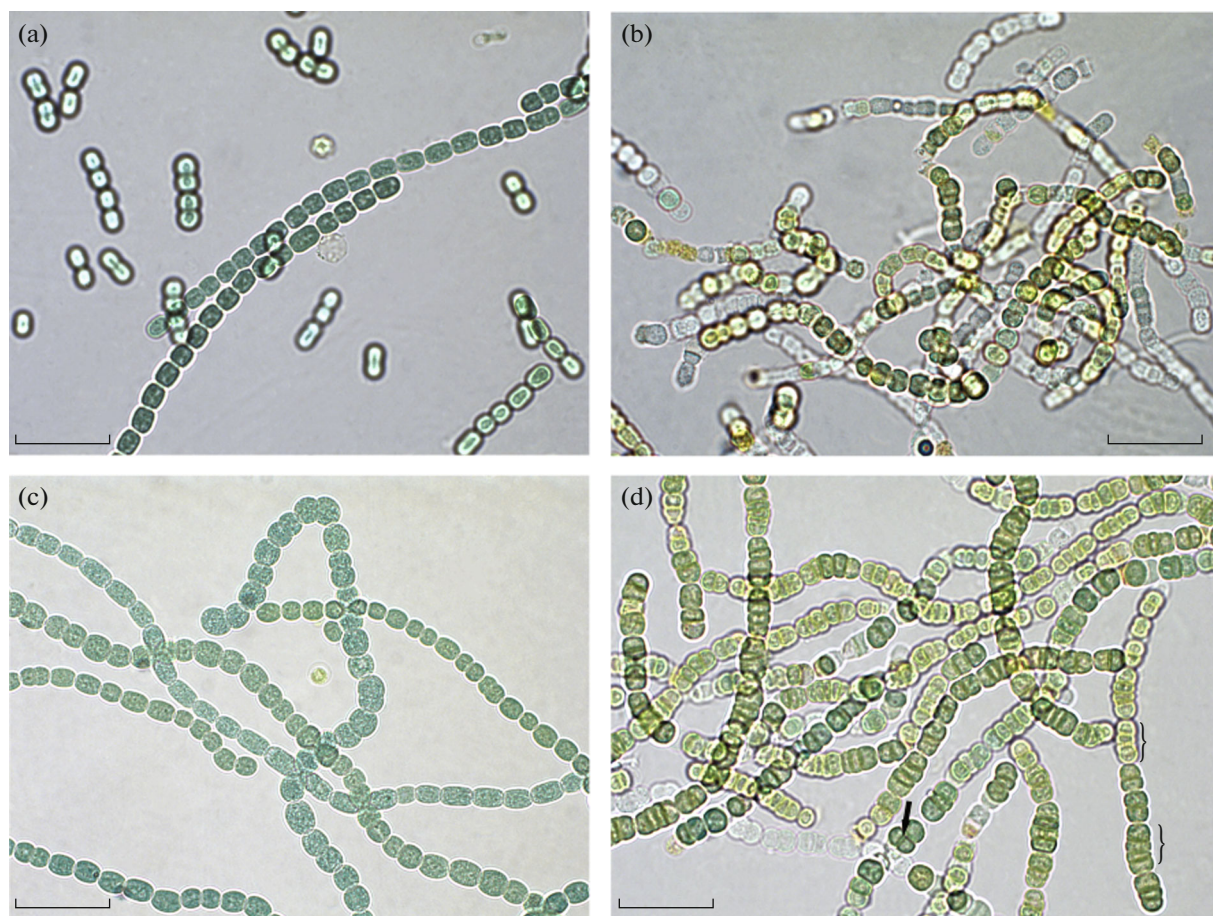


**Fig. 3.** Bright-field micrographs of (a, b) *Nostoc* sp. PCC 7118 and (c, d) *Nostoc* sp. PCC 7120 cultures incubated in (a, c) the complete and (d, e) P-free medium for 11 days. The curly brackets mark a group of disk-shaped cells, the arrow points at a group of anomalously dividing cells. Scale bars: 20  $\mu\text{m}$ .

both studied strains (Figs. 4c, 4d, 4g, 4h). These rearrangements included: (1) a decrease in the electron density of the cytosol which varied in the magnitude over the section plane; (2) a reduction in the length and number of thylakoids that lost their collinearity and did not exhibit stress-induced lumen expansion; (3) a sharp reduction in the area of nucleoid zones and the abundance of ribosomes; (4) reduced abundance and size of carboxysomes; (5) changes in the abundance and size of inclusions of reserve polymers (disappearance of glycogen granules and expansion of CG). Despite the similarity of the ultrastructural reorganizations in both strains, there were certain differences in the retention of phycobilisomes and PolyP, as well as in the quantitative parameters of reserve polymer inclusions (Fig. 5).

The cells of both cultures grown in BG-11 medium revealed the presence of carboxysomes in almost all studied cell sections (Figs. 4a, 4b, 4e, 4f and 5), at the same time, the number of carboxysomes per cell section in PCC 7120 was slightly higher than that in PCC 7118 (Fig. 5a). With prolonged P starvation, the number and total area of carboxysomes on the cell sections

of both strains significantly decreased, and in PCC 7118 to a greater extent than in PCC 7120 (Figs. 5b, 5c).

Granules of poly- $\beta$ -hydroxybutyrate (Phb) in PCC 7118 cells grown in the complete medium were more ample than in PCC 7120 (Figs. 5a, 5b). At the same time, the proportion of the area occupied by Phb on the cell sections of the P-starved cells in PCC 7118 decreased more than 20 times, a prolonged P starvation induced only a modest (10%) decline in this parameter.

In both studied cultures, the presence of lipid  $\beta$ -granules was noted in all cultivation variants. Their number and total area in PCC 7118 cell sections was independent of the presence of P in the medium (Figs. 5b, 5c). In PCC 7120, on the contrary, these parameters of  $\beta$ -granules increased almost twice during P starvation (Figs. 5b, 5c).

The studied strains showed significant differences in the accumulation of CG when grown in the complete medium. The CG number in PCC 7120 was more than two times higher than in PCC 7118

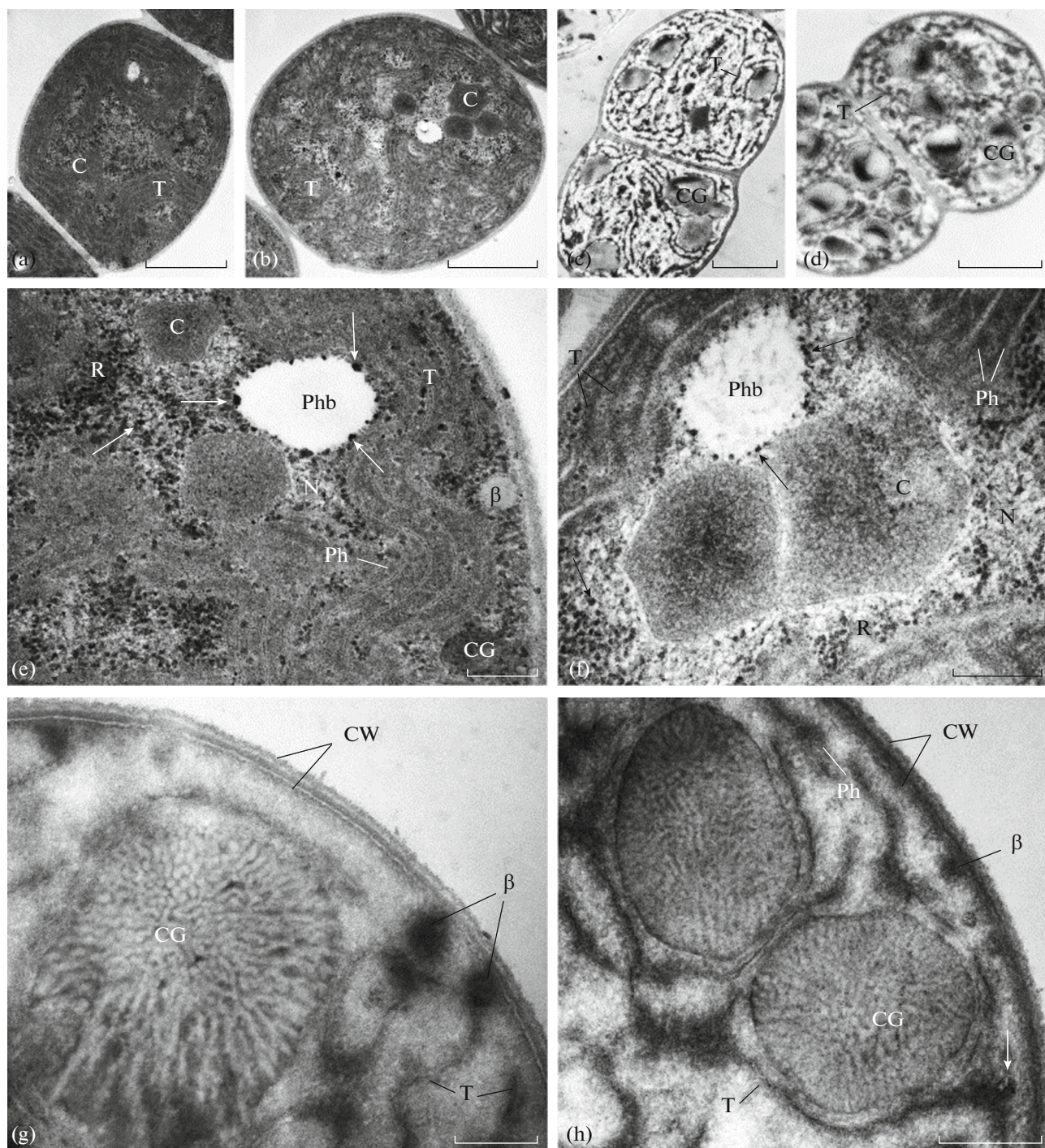


**Fig. 4.** Ultrastructure of the vegetative cells of the cyanobacteria *Nostoc* sp. PCC 7118 (a, c, e, g) and *Nostoc* sp. PCC 7120 (b, d, f, h), cultivated (a, b, e, f) in complete BG-11 medium or in the BG-11-P medium (c, d, g, h). C—carboxysome; CW—cell wall; N—nucleoid zone; Phb—poly-β-hydroxybutyrate granule, R—ribosomal clusters; T—thylakoid(s); Ph—phycobilisomes; CG—cyanophycin granule; β—lipid β-granules; arrows point at PolyP (see also Ismagulova et al., 2018). Scale bars: 1 μm (a–d) and 0.2 μm (e–h).

(Fig. 5b). After prolonged P starvation, massive accumulation of CG was noted in both cultures, their abundance increased fourfold in PCC 7118 and five times in PCC 7120, while the difference in the amount of CG between the cultures increased almost 3 times.

The variation of CG total area on the cell sections was even higher (Figs. 5b, 5c).

The differences between the studied strains in the accumulation of PolyP also turned out to be significant. In the cells of PCC 7120, PolyP was found to be

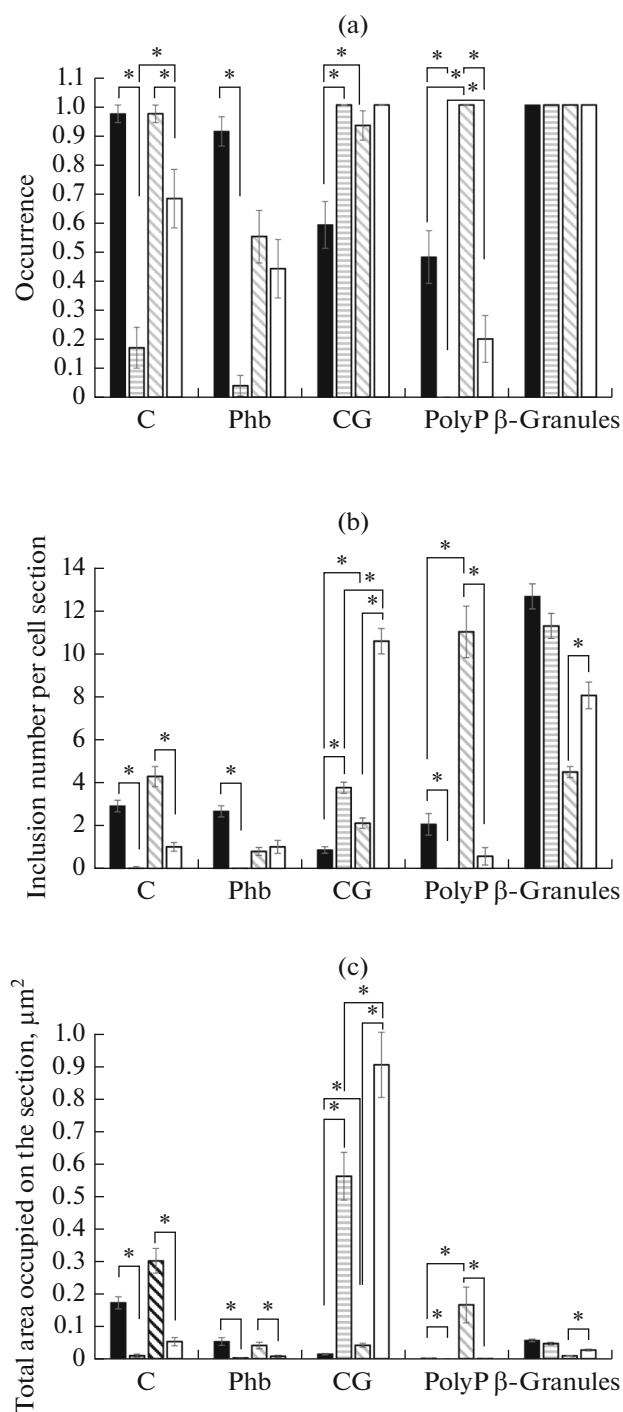


**Fig. 5.** Changes of (a) occurrence, (b) abundance, and (c) total area of caboxysomes (C), polyphosphate (PolyP), cyanophycin (CG), poly-β-hydroxybutyrate (Phb), lipid granules (β-granules) on cell sections of *Nostoc* sp. PCC 7118 (■, ▨) and *Nostoc* sp. PCC 7120 (□, ▩) cultivated in complete (BG-11; ■, ▨) or P-free medium (BG-11-P; ▨, □). Average values ± SE are shown. The values different at the significance level of  $p \leq 0.05$  are marked with brackets and asterisks (\*).

significantly higher than in PCC 7118 grown in complete medium (Figs. 5b, 5c). PolyP was also detected on all cell sections in PCC 7120 and only on half of the analyzed cell sections in PCC 7118 (Fig. 5a). After prolonged P starvation (18 days for PCC 7118), PolyP was not detected on PCC 7118 cell sections, while in PCC 7120, traces of PolyP were retained for up to 27 days.

Overall, the prolonged P starvation led to the disappearance of PolyP reserves in PCC 7118 cells, as well as to a significant reduction in their carbon reserves (C, Phb), while PCC 7120 accumulated more PolyP and spent them more slowly during prolonged P starvation.

The morphometry of phycobilisomes on the cell sections of the studied cyanobacterial strains revealed their fundamental difference in the degree of retention of the light-harvesting antenna during P starvation (Fig. 6). Phycobilisomes which were localized on the cytoplasmic surface of the thylakoids, looked like segments of a circle on the cell sections (Figs. 4e, 4f). The width of the phycobilisomes measured at their contact with the membrane always exceeded their height (the elevation above the thylakoid plane). Prolonged P starvation triggered approximately a twofold decrease in the height and width of phycobilisomes in PCC 7118, while in PCC 7120 this was not the case (Fig. 6).

**Profiling of the expression of genes involved in P metabolism.** P starvation changed the expression levels of certain genes (Table 2) involved in the uptake of  $P_i$  by the cell and its metabolism, including the metabolism of PolyP. Particularly, genes encoding polyphosphate kinase 1—*ppk1*, the central enzyme of PolyP biosynthesis, were selected as targets (Sanz-Luke et al., 2020) as well as exopolyphosphatase *ppx* and pyrophosphatase *ppa* involved in the hydrolysis of PolyP (Gomez-Garcia et al., 2003; Hiyoshi et al., 2021) and the genes of PolyP-dependent kinases—polyphosphate kinase 2, *ppk2* (Dzeso et al., 2002), and polyphosphate glucokinase, *ppgk* (Klemke et al., 2014). The expression levels of two genes from the *pstS* family encoding subunits of periplasmic  $P_i$  transporters (*pst1* and *pst2*) were also determined. One of them, *pst1* is a part of Pho regulon upregulated by  $P_i$  shortage (Su et al., 2007).

The greatest differences in the expression of P metabolism-related genes in PCC 7118 and PCC 7120 were recorded after 2 days of incubation in a P-free medium. At the same time, the induction of *ppk1* expression took place only in PCC 7120, and the *ppx* expression was induced only in PCC 7118. Simultaneous induction of *ppx* and *ppa* genes was not observed, but these data are consistent with a greater abundance of PolyP in PCC 7120 as compared to PCC 7118 (Fig. 5).

The most extensive changes at the onset of P starvation were observed in the expression of the genes of the periplasmic  $P_i$  transporters, *pstS1* and *pstS2*. Thus, the expression of *pstS1* increased by an order of magnitude, and in PCC 7120 the expression level of this gene was 3–5 times higher than in PCC 7118 (Table 2).

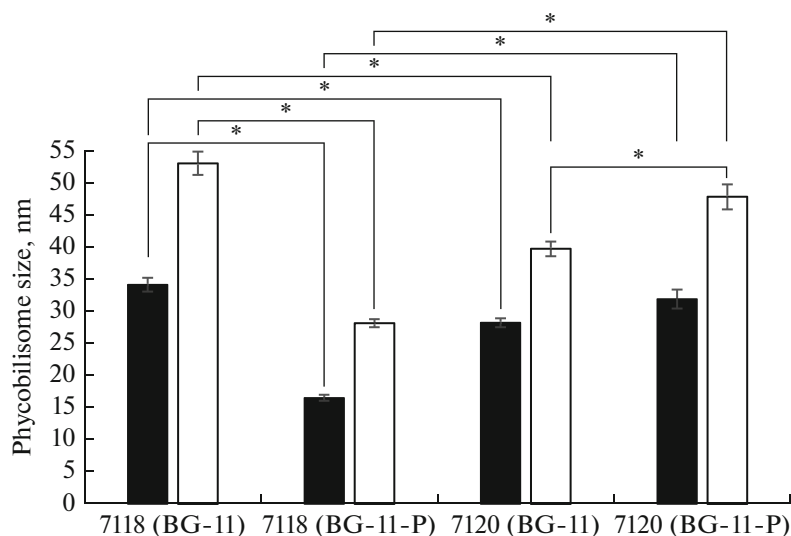


**Fig. 6.** Height (■) and base width (□) of phycobilisomes in the cells of *Nostoc* sp. PCC 7118 and *Nostoc* sp. PCC 7120 incubated in the complete (BG-11) or P-free (BG-11-P) medium for 18 or 27 days, respectively. Average values  $\pm$  SE are shown. The values different at the significance level of  $p \leq 0.05$  are marked with brackets and asterisks (\*).

However, *pstS2* turned out to be the more inducible  $P_i$  transporter gene under our experimental conditions: its expression increased by an order of magnitude in PCC 7118 and more than 400 times in PCC 7120.

With depletion of the intracellular reserves of P, accompanied by cessation of cell division and biomass

accumulation (Fig. 1), PCC 7118 and PCC 7120 showed similar levels of *ppk1* gene expression (twofold induction), *pstS1* (30–40-fold induction), and *pstS2* (125-fold induction). During P starvation, the expression of the genes of PolyP-dependent kinases, *ppgk* and *ppk2*, was 1.5–2 times higher in PCC 7120 than in PCC 7118.

**Table 2.** Differential expression of genes involved in the uptake of  $P_i$  and metabolism of P during P starvation of *Nostoc* sp. PCC 7118 and *Nostoc* sp. PCC 7120

Target gene	PCC 7118		PCC 7120	
	days of P starvation			
	2	11	2	11
Pyrophosphatase, <i>ppa</i> (all3570*)	0.262*	0.904	1.805	0.421
	0.269*	0.845	1.783	0.610
Polyphosphate kinase 1, <i>ppk1</i> (alr3593)	1.031	2.684	2.730	1.820
	0.928	2.133	3.069	1.890
Polyphosphate kinase 2, <i>ppk2</i> (all2088)	0.214	0.612	0.689	0.742
	0.207	0.398	0.589	0.665
Exopolyphosphatase, <i>ppx</i> (all3552)	3.946	1.129	0.964	0.427
	3.443	1.109	1.126	0.670
Polyphosphate glucokinase, <i>ppgk</i> (all1371)	0.884	0.510	1.882	1.245
	0.777	0.542	0.955	0.893
$P_i$ -transporter, <i>pstS1</i> (all4575)	7.937	29.0	27.95	38.40
	4.875	29.80	28.87	44.40
$P_i$ -transporter, <i>pstS2</i> (all0911)	22.40	126.5	512.82	124.95
	11.987	170.2	436.48	115.09

\* The results of two independent experiments are shown for each sample.

## DISCUSSION

Closely related organisms whose phenotypes differ in a certain essential feature constitute a useful model for mechanistic studies of phenotypic implementation and molecular regulation of this trait. Such model systems include the pair of strains PCC 7120 and PCC 7118 of cyanobacteria *Nostoc* sp. These strains differ in their ability to form mature heterocysts and, consequently, in their capability of diazotrophy under aerobic conditions (Elhai and Wolk, 1990; Sato and Wada, 1996; Kaneko, 2001; Sato et al., 2012). Of particular interest in this context are the effects of variable P availability, which is among the main factors limiting diazotrophy in cyanobacteria (Raven, 2008). Here, we tackled this problem by looking for inter-strain differences in the PCC 7120 and PCC 7118 strain pair in response to P starvation under non-diazotrophic conditions.

The study revealed significant differences in growth kinetics, ultrastructural cell reorganization, and the expression profile of genes involved in P metabolism during P starvation though both strains showed typical stress responses of phototrophic microorganisms as well. In most cases, P starvation causes a decrease in the concentration of total protein, chlorophyll, ribosomal and messenger RNA (see e.g. Berdalet et al., 1994). A decrease in the abundance of ribosomes and/or the expression of genes encoding their components was observed in chlorophytes such as *Chlamydomonas reinhardtii* (Grossman and Takahashi, 2001) and diatoms such as *Thalassiosira pseudonana* (Dyhrman et al., 2012), and cyanobacteria e.g. *Synechococcus* sp. WH8102 (Tetu et al., 2009). An uneven decrease in the electron density of the cytosol on cell sections indicates a decrease or non-uniform degradation of soluble cellular proteins and small sub-cellular structures.

P starvation also leads to a reallocation of carbon and other element fluxes between cell subcompartments and depots. Its consequences include the ultrastructural reorganization of the cell, which was observed in the present study. The nature of these changes depends both on the intensity of the stressor (the duration of P starvation) and on the level of tolerance to this stressor. Thus, in both studied strains prolonged P starvation induced a drastic decrease in the abundance of carboxysomes, glycogen granules, PolyP, Phb, ribosomes, a reduction in the size of nucleoid zones, thylakoids and phycobilisomes. In certain cases (e.g. *Microcystis aeruginosa*) carboxysomes disappeared on the 20th day of P starvation (Barlow et al., 1979). However, some lines of evidence suggest that carboxysomes persist during P starvation (Allen, 1984). Genes encoding small and large RuBisCO subunits are repressed under these conditions (Solovchenko et al., 2020), but dissolved RuBisCO can remain in cells (Allen, 1984) so the assimilation of inorganic carbon remains possible in the absence of carboxysomes.

The abundance of certain inclusion types (glycogen, PolyP, Phb) decreased until complete disappearance on the background of “hyperaccumulation” of cyanophycin in the vegetative cells. Normally, cyanophycin accumulation is a feature of the cells in the state of unbalanced growth, for example, in nitrogen-sufficient cells lacking sulfur, P, or light energy (Allen, 1984; Flores et al., 2019). A significant increase in cyanophycin biosynthesis requires a high intracellular concentration of L-arginine and L-aspartic acid (Allen, 1984; Stephan et al., 2000; Maheswaran et al., 2006; Flores et al., 2019). Protein catabolism can supply arginine and aspartate (Allen and Hawley, 1983), so salvaging of soluble proteins can be a source of amino acids for cyanophycin buildup in stationary-phase cultures (Simon, 1973). As noted above, P-starving PCC 7118 and 7120 cells had mostly electron-transparent cytosol, apparently due to depletion of soluble proteins (Berdalet et al., 1994).

In the context of cyanophycin accumulation, arginine biosynthesis is of great importance. Thus, *Nostoc ellipsosporum* harbors genes *argC* and *argL* encoding the enzymes of arginine biosynthesis. The gene *argC* is associated with the biosynthesis of arginine incorporated into proteins, and the *argL* gene is responsible for arginine supply to be incorporated into cyanophycin (Leganés et al., 1998). Cyanophycin accumulation in *Synechocystis* sp. PCC 6803 is regulated by the proportion of L-arginine in the total nitrogen pool (Stephan et al., 2000). The key enzyme in arginine biosynthesis is *N*-acetyl-L-glutamate kinase (NAGK). It is activated by PII protein-related signals. Non-phosphorylated complexes of the PII-MgATP trimer bind strongly to NAGK, increasing its enzymatic activity (Forchhammer and Lüddecke, 2016; Flores et al., 2019). This leads to the synthesis of a large amount of arginine, which can be incorporated into cyanophycin (Maheswaran et al., 2006). Thus, activation of arginine synthesis via PII may play a role in cyanophycin accumulation, while PII participates in controlling cyanophycin synthesis (Heinrich et al., 2004). One can think that P starvation reduces the level of phosphorylation of PII, thereby stimulating the accumulation of cyanophycin. At the same time, activation of cyanophycin synthetase expression is also necessary to implement this response. We have previously shown that at least one of the genes (*cphA1*) encoding cyanophycin synthetase was activated in P-starved cells (Solovchenko et al., 2020).

P starvation increased the cyanophycin content in cells of other cyanobacteria species e.g., *Aphanocapsa* sp. 6308 (Allen and Weathers, 1980), *Agmenellum quadruplicatum* (Stevens Jr. et al., 1981), *Synechocystis* sp. PCC 6803 (Stephan et al., 2000), *M. aeruginosa* (Barlow et al., 1979). It is conceivable that the mass accumulation of cyanophycin is because this compound contains both nitrogen and carbon. Accordingly, it is a suitable depot for storing excess nitrogen and carbon released during P starvation which shrinks the meta-

bolic sink for these elements. Notably, this effect may be of great importance for biotechnology, since cyanophycin is a valuable bio product of cyanobacteria (Du et al., 2019).

The studied strains significantly differed in the accumulation of PolyP when  $P_i$  was ample: when cultured in the complete medium, PCC 7120 harbored much more PolyP than PCC 7118 (Fig. 5). It is also interesting that PolyP disappeared from the sections of PCC 7118 cells by the 18th day of P starvation, while in PCC 7120 traces of PolyP persisted even on the 27th day of P starvation.

In parallel with the onset of cellular metabolism quiescence, there was a reduction of the PSA, manifested by dismantling of the thylakoid membranes and a decrease in photosynthetic pigments, mainly those of the light-harvesting antenna. As in our experimental conditions, the number of thylakoids decreased in *M. aeruginosa* after 20 days of P starvation, and they reoriented perpendicular to the cell wall (Barlow et al., 1979). In chlorophyte *Chlorella vulgaris*, 17 days of P starvation caused the reduction of chloroplasts (Sun et al., 2019). Previously, we showed that on day 11 of P starvation, PCC 7118 cells displayed a pronounced reduction of PSA and a decrease in chlorophyll content while carotenoids were retained (Solovchenko et al., 2020). Similarly, P starvation caused a decrease in the chlorophyll content in *A. quadruplicatum* (Stevens Jr. et al., 1981) and in *Synechococcus* sp. PCC 7942 (Collier et al., 1994); in the latter, a decrease in  $\beta$ -carotene and photosystem II activity were also documented. *Synechocystis* sp. PCC 6803 also showed marked degradation of thylakoid membranes with partial loss of pigments and photosynthetic activity (Stephan et al., 2000).

These phenomena are observed in the cells deprived of not only P, but also other mineral nutrients, such as nitrogen, iron, sulfur, etc. At the same time, the number of phycobiliproteins in cells decreases, phycobilisomes degrade and even disappear completely (Bryant, 1986; Wanner et al., 1986). It is believed that the reduction of the phycobin antenna begins with the proteolysis of phycocyanin from the side cylinders (Sherman et al., 2000), while the more stable allophycocyanin core degrades more slowly. The ultrastructural pattern of phycobilisome reduction during P starvation in our experiments aligns well with these concepts. Thus, Fig. 6 clearly shows an almost twofold decrease in the size of phycobilisomes in the P-starving PCC 7118 cells, while in PCC 7120 the sizes of these structures did not change even after prolonged P starvation (Figs. 4, 6). The abundance of phycobilisomes decreased synchronously with the decline in chlorophyll during P starvation-induced disassembly of thylakoids (Fig. 2). Previously, we showed that in the course of P starvation, the expression of genes encoding phycobilisome proteins decreases sharply (Solovchenko et al., 2020), similar

data were obtained for other cyanobacteria such as *A. quadruplicatum* (Stevens Jr. et al., 1981) and *Synechococcus* sp. PCC 7942 (Collier et al., 1994).

In our experiments, lumen was not detected in thylakoids undergoing dismantling meaning that the thylakoids lost their functional response to P starvation. In contrast, *Plectonema boryanum* cells possessed an extensive intra-thylakoid space after 5 days of P starvation (Jensen and Sicko, 1974). A decrease in the electron density of inter-thylakoid regions was also observed during P starvation of *A. quadruplicatum* (Stevens Jr. et al., 1981).

In general, the ultrastructural reorganization of the cell caused by P starvation was more profound in PCC 7118 than in PCC 7120. Thus, PCC 7118 demonstrated a decrease in the proportion of carboxysomes and an increase in the proportion of cyanophycin in the proplast area by 12.5 and 75 times, and PCC 7120—only by 5 and 27 times, respectively (Figs. 4, 5). Our findings suggest that the ability of the PCC 7120 to accumulate reserves of P, which was an order of magnitude higher than that of PCC 7118, largely explains the relatively higher resilience of PCC 7120 to P starvation. Other researchers have also noted this ability of PCC 7120 to accumulate PolyP (Trentin et al., 2023).

For a more confident interpretation and deeper understanding of the nature of the aforementioned changes in the PCC 7118 phenotype vs. PCC 7120 caused by P starvation, we studied the expression of key genes involved in P metabolism (Table 2). A comparative analysis of expression profiles revealed several features characteristic of the model pair of strains “PCC 7118–PCC 7120.” Thus, we did not find the simultaneous induction of the *ppx* and *ppa* genes, characteristic of another model strain *Synechocystis* sp. PCC 6803 (Gómez-García et al., 2003), but these findings are consistent with a large abundance of PolyP in PCC 7120 compared to PCC 7118 (Fig. 5). It is also likely that the mobilization of intracellular PolyP reserves in PCC 7120 occurs with the participation of pyrophosphatase *ppa* catalyzing the hydrolysis of inorganic pyrophosphate; the expression of the gene increased 1.8 times. However, the largest changes at the beginning of P starvation were observed in the expression of the genes *pstS1* and *pstS2* encoding the subunits of the periplasmic  $P_i$  transporters *pst1* and *pst2* (Pitt et al., 2010). Apparently, during P starvation the main  $P_i$  transporter in the PCC 7118 and PCC 7120 model strains is *pst2*, with the dramatic increase in the *pstS2* expression, but PCC 7120 is almost 40 times ahead of PCC 7118 in this parameter. Still, the mechanism of *pst2* induction remains unclear: this *pts2* operon is located outside of the Pho-regulon in PCC 7120, but, like *pst1*, it participates in the early response to P starvation.

Collectively, the obtained data suggests that the phenotypic differences between the strains *Nostoc* sp. PCC 7118 and PCC 7120 are not limited to the differ-

ent ability to form heterocysts. These strains demonstrate different responses to stressors, such as P starvation, under conditions that do not trigger diazotrophy. Our results are in line with the work of Bozan et al. (2022) who conducted a comparative study of closely related strains of cyanobacteria *Tolypothrix* sp. PCC 7712 and *Tolypothrix* sp. PCC 7601 (often called *Fremyella diplosiphon*). Despite the significant similarity at the genome level, PCC 7712 was able to fix N<sub>2</sub>, whereas PCC 7601 showed neither nitrogenase activity nor the ability to form heterocysts. This is surprising, since the PCC 7601 genome encodes all the necessary proteins involved in nitrogen fixation (Bozan et al., 2022). To summarize, a deeper understanding of possible drivers of the phenotypic diversity of stress responses in near-isogenic strains would require a comparative analysis of their whole-genome sequences. It is necessary since even a single gene rupture or alteration of its genomic context can result in different physiological response(s). Moreover, the diversity of stress responses can stem from the pleiotropic effect of single-gene changes (Koksharova et al., 2007; Gorelova et al., 2013). In other words, similarity of genomes of the organisms might not entail a similarity in their physiology.

A comparative analysis of the responses of PCC 7118 and PCC 7120 to the combined stress (nitrogen and P starvation) is planned for the near future. It would allow to gain a deeper insight into the mechanisms of stress tolerance in PCC 7118 and PCC 7120 and improve our understanding of the modulation of the cyanobacteria production process by nitrogen and P availability in aquatic ecosystems and industrial cultivation systems. We believe that these findings will help the scientists and practitioners to harness the biotechnological potential of cyanobacteria.

#### ACKNOWLEDGMENTS

The TEM studies were carried out at Moscow State University Shared User Facilities “Electron microscopy in life sciences.”

#### FUNDING

This work was supported by the Russian Science foundation (grant 21-74-20004).

#### ETHICS APPROVAL AND CONSENT TO PARTICIPATE

This work does not contain any studies involving human and animal subjects.

#### CONFLICT OF INTEREST

The authors of this work declare that they have no conflicts of interest.

#### REFERENCES

- Allen, M. and Hawley, M.A., Protein degradation and synthesis of cyanophycin granule polypeptide in *Aphanocapsa* sp., *J. Bacteriol.*, 1983, vol. 154, no. 3, pp. 1480–1484.
- Allen, M.M., Cyanobacterial cell inclusions, *Annu. Rev. Microbiol.*, 1984, vol. 38, no. 1, pp. 1–25.
- Allen, M.M. and Weathers, P.J., Structure and composition of cyanophycin granules in the cyanobacterium *Aphanocapsa* 6308, *J. of Bacteriol.*, 1980, vol. 141, no. 2, pp. 959–962.
- Barlow, D.J., van Rensburl, W., Pieterse, A., and Eloff, J., Effect of phosphate concentration on the fine structure of the cyanobacterium, *Microcystis aeruginosa* Kütz. emend. Elenkin, *J. Limnol. Soc. South. Africa*, 1979, vol. 5, no. 2, pp. 79–83.
- Bennett, E. and Elser, J., A broken biogeochemical cycle, *Nature*, 2011, vol. 478, pp. 29–31.
- Berdalet, E., Latasa, M., and Estrada, M., Effects of nitrogen and phosphorus starvation on nucleic acid and protein content of *Heterocapsa* sp., *J. Plankton Res.*, 1994, vol. 16, no. 4, pp. 303–316.
- Blank, L.M., The cell and P: from cellular function to biotechnological application, *Curr. Opin. Biotechnol.*, 2012, vol. 23, no. 6, pp. 846–851.
- Bozan, M., Popp, D., Kallies, R., da Rocha, U.N., Klähn, S., and Bühler, K., Whole-genome sequence of the filamentous diazotrophic cyanobacterium *Tolypothrix* sp. PCC 7712 and its comparison with non-diazotrophic *Tolypothrix* sp. PCC 7601, *Front. Microbiol.*, 2022, vol. 13, p.1042437.
- Bryant, D., The cyanobacterial photosynthetic apparatus: comparison to those of higher plants and photosynthetic bacteria, *Can. Bull. Fish. Aquat. Sci.*, 1986, vol. 214, pp. 423–500.
- Canavate, J.P., Armada, I., and Hachero-Cruzado, I., Aspects of phosphorus physiology associated with phosphate-induced polar lipid remodelling in marine microalgae, *J. Plant Physiol.*, 2017, vol. 214, pp. 28–38.
- Chen, M. and Graedel, T., A half-century of global phosphorus flows, stocks, production, consumption, recycling, and environmental impacts, *Global Environ. Change*, 2016, vol. 36, pp. 139–152.
- Collier, J.L. and Grossman, A., Chlorosis induced by nutrient deprivation in *Synechococcus* sp. strain PCC 7942: not all bleaching is the same, *J. Bacteriol.*, 1992, vol. 174, no. 14, pp. 4718–4726.
- Collier, J.L., Herbert, S.K., Fork, D.C., and Grossman, A.R., Changes in the cyanobacterial photosynthetic apparatus during acclimation to macronutrient deprivation, *Photosynth. Res.*, 1994, vol. 42, no. 3, pp. 173–183.
- Cordell, D. and White, S., Life’s bottleneck: implications of global phosphorus scarcity and pathways for a sustainable food system, *Annu. Rev. Environ. Resour.*, 2014, vol. 39, pp. 161–188.
- Daneshgar, S., Callegari, A., Capodaglio, A., and Vaccari, D., The potential phosphorus crisis: resource conservation and possible escape technologies: a review, *Resources*, 2018, vol. 7, no. 2, p. 37.
- Du, J., Li, L., and Zhou, S., Microbial production of cyanophycin: from enzymes to biopolymers, *Biotechnol. Adv.*, 2019, vol. 37, no. 7, p. 107400.

- Dyhrman, S.T., Nutrients and their acquisition: phosphorus physiology in microalgae, in *The Physiology of Microalgae*, 2016, pp. 155–183.
- Dyhrman, S.T., Jenkins, B.D., Rynearson, T.A., Saito, M.A., Mercier, M.L., Alexander, H., Whitney, L.P., Drzewianowski, A., Bulygin, V.V., Bertrand, E.M., Wu, Z., Benitez-Nelson, C., and Heithoff, A., The transcriptome and proteome of the diatom *Thalassiosira pseudonana* reveal a diverse phosphorus stress response, *PLoS One*, 2012, vol. 7, no. 3, p. e33768.
- Elhai, J. and Wolk, C.P., Developmental regulation and spatial pattern of expression of the structural genes for nitrogenase in the cyanobacterium *Anabaena*, *The EMBO J.*, 1990, vol. 9, no. 10, pp. 3379–3388.
- Flores, E., Arévalo, S., and Burnat, M., Cyanophycin and arginine metabolism in cyanobacteria, *Algal Res.*, 2019, vol. 42, p. 101577.
- Forchhammer, K. and Lüddecke, J., Sensory properties of the PII signalling protein family, *The FEBS J.*, 2016, vol. 283, no. 3, pp. 425–437.
- Gómez-García, M.R., Losada, M., and Serrano, A.J.B., Concurrent transcriptional activation of ppa and ppx genes by phosphate deprivation in the cyanobacterium *Synechocystis* sp. strain PCC 6803, *Biochem. Biophys. Res. Commun.*, 2003, vol. 302, no. 3, pp. 601–609.
- Gorelova, O., Baulina, O., Rasmussen, U., and Koksharova, O., The pleiotropic effects of ftn2 and ftn6 mutations in cyanobacterium *Synechococcus* sp. PCC 7942: an ultrastructural study, *Protoplasma*, 2013, vol. 250, pp. 931–942.
- Gorelova, O., Baulina, O., Solovchenko, A., Chekanov, K., Chivkunova, O., Fedorenko, T., and Lobakova, E., Similarity and diversity of the *Desmodesmus* spp. microalgae isolated from associations with White Sea invertebrates, *Protoplasma*, 2015, vol. 252, pp. 489–503.
- Gross, M., Where is all the phosphorus?, *Curr. Biol.*, 2017, vol. 27, no. 21, pp. R1141–R1144.
- Grossman, A. and Takahashi, H., Macronutrient utilization by photosynthetic eukaryotes and the fabric of interactions, *Annu. Rev. Plant Biol.*, 2001, vol. 52, no. 1, pp. 163–210.
- Grossman, A.R. and Aksoy, M., Algae in a phosphorus-limited landscape, *Annual Plant Reviews*, Vol. 48: *Phosphorus Metabolism in Plants*, 2015, pp. 337–374.
- Heinrich, A., Maheswaran, M., Ruppert, U., and Forchhammer, K., The *Synechococcus elongatus* PII signal transduction protein controls arginine synthesis by complex formation with N-acetyl-l-glutamate kinase, *Mol. Microbiol.*, 2004, vol. 52, no. 5, pp. 1303–1314.
- Hiyoshi, T., Oyanagi K., Niki, T., Fujiwara, S., and Sato, N., Requirement of the exopolyphosphatase gene for cellular acclimation to phosphorus starvation in a cyanobacterium *Synechocystis* sp. PCC 6803, *Biochem. Biophys. Res. Commun.*, 2021, vol. 540, pp. 16–21.
- Ishige, K., Zhang, H., and Kornberg, A., Polyphosphate kinase (PPK2), a potent, polyphosphate-driven generator of GTP, *Proc. Natl. Acad. Sci. U. S. A.*, 2002, vol. 99, no. 26, pp. 16684–16688.
- Ismagulova, T., Shebanova, A., Gorelova, O., Baulina, O., and Solovchenko, A., A new simple method for quantification and locating P and N reserves in microalgal cells based on energy-filtered transmission electron microscopy (EFT-EM) elemental maps, *PLoS One*, 2018, vol. 13, no. 12, p. e0208830.
- Jämsä, M., Lynch, F., Santana-Sánchez, A., Laaksonen, P., Zaitsev, G., Solovchenko, A., and Allah-verdiyeva, Y., Nutrient removal and biodiesel feedstock potential of green alga UHCC00027 grown in municipal wastewater under Nordic conditions, *Algal Res.*, 2017, vol. 26, pp. 65–73.
- Jensen, T.E. and Sicko, L.M., Phosphate metabolism in blue-green algae. I. Fine structure of the “polyphosphate overplus” phenomenon in *Plectonema boryanum*, *Can. J. Microbiol.*, 1974, vol. 20, no. 9, pp. 1235–1239.
- Kaneko, T., Complete genomic sequence of the filamentous nitrogen-fixing cyanobacterium *Anabaena* sp. strain PCC 7120, *DNA Res.*, 2001, vol. 8, pp. 205–213.
- Klemke, F., Beyer, G., Sawade, L., Saitov, A., Korte, T., Maldener, I., Lockau, W., Nürnberg, D.J., and Volkmer, T., All1371 is a polyphosphate-dependent glucokinase in *Anabaena* sp. PCC 7120, *Microbiology (SGM)*, 2014, vol. 160, Pt. 12, p. 2807.
- Koksharova, O., Klint, J., and Rasmussen, U., Comparative proteomics of cell division mutants and wild type of *Synechococcus* sp. strain PCC 7942, *Microbiology (SGM)*, 2007, vol. 153, pp. 2505–2517.
- Kulaev, I., Vagabov, I., and Kulakovskaya, T., *The Biochemistry of Inorganic Polyphosphates*, Chichester: Wiley, 2004.
- Leganés, F., Fernandez-Pinas, F., and Wolk, C., A transposition-induced mutant of *Nostoc ellipsosporum* implicates an arginine-biosynthetic gene in the formation of cyanophycin granules and of functional heterocysts and akinetes, *Microbiology (SGM)*, 1998, vol. 144, no. 7, pp. 1799–1805.
- Ludwig, M. and Bryant, D.A., Acclimation of the global transcriptome of the cyanobacterium *Synechococcus* sp. strain PCC 7002 to nutrient limitations and different nitrogen sources, *Front. Microbiol.*, 2012, vol. 3, p. 145.
- Maheswaran, M., Ziegler, K., Lockau, W., Hagemann, M., and Forchhammer, K., PII-regulated arginine synthesis controls accumulation of cyanophycin in *Synechocystis* sp. strain PCC 6803, *J. Bacteriol.*, 2006, vol. 188, no. 7, pp. 2730–2734.
- Merzlyak, M.N. and Naqvi, K.R., On recording the true absorption spectrum and the scattering spectrum of a turbid sample: application to cell suspensions of the cyanobacterium *Anabaena variabilis*, *J. Photochem. Photobiol. B*, 2000, vol. 58, nos. 2–3, pp. 123–129.
- Muhlroth, A., Winge, P., El Assimi, A., Jouhet, J., Marechal, E., Hohmann-Marriott, M.F., Vadstein, O., and Bones, A.M., Mechanisms of phosphorus acquisition and lipid class remodeling under P limitation in a marine microalga, *Plant Physiol.*, 2017, vol. 175, no. 4, pp. 1543–1559.
- Nesbitt, J., Removal of phosphorus from municipal sewage plant effluents, *Eng. Res. Bull.*, 1966.
- Parshina, E.Y., Liu, W., Yusipovich, A., Gvozdev, D.A., He, Y., Pirutin, S.K., Klimanova, E.A., Maksimov, E.G., and Maksimov, G.V., Spectral and conformational characteristics of phycocyanin associated with changes of medium pH, *Photosynth. Res.*, 2024, pp. 1–11.
- Pitt, F.D., Mazard, S., Humphreys, L., and Scanlan, D.J., Functional characterization of *Synechocystis* sp. strain PCC 6803 pst1 and pst2 gene clusters reveals a novel strategy for

- phosphate uptake in a freshwater cyanobacterium, *J. Bacteriol.*, 2010, vol. 192, no. 13, pp. 3512–3523.
- Raven, J.A., Phosphorus and the future, in *The Ecophysiology of Plant-Phosphorus Interactions*, Dordrecht: Springer, 2008, pp. 271–283.
- Reynolds, E., The use of lead citrate at high pH as an electron-opaque stain in electron microscopy, *J. Cell Biol.*, 1963, vol. 17, no. 1, p. 208.
- Sanz-Luque, E., Bhaya, D., and Grossman, A.R., Polyphosphate: a multifunctional metabolite in cyanobacteria and algae, *Front. Plant Sci.*, 2020, vol. 11, p. 938.
- Sato, N., Moriyama, T., Toyoshima, M., Mizusawa, M., and Tajima, N., The all0458/lti46.2 gene encodes a low temperature-induced Dps protein homologue in the cyanobacteria *Anabaena* sp. PCC 7120 and *Anabaena variabilis* M3, *Microbiology* (SGM), 2012, vol. 158, no. 10, pp. 2527–2536.
- Sato, N. and Wada, A., Disruption analysis of the gene for a cold-regulated RNA-Binding protein, rbpA1, in *Anabaena*: cold-induced initiation of the heterocyst differentiation pathway, *Plant Cell Physiol.*, 1996, vol. 37, pp. 1150–1160.
- Sherman, D.M., Tucker, D., and Sherman, L.A., Heterocyst development and localization of cyanophycin in N<sub>2</sub>-fixing cultures of *Anabaena* sp. PCC 7120 (Cyanobacteria), *J. Phycol.*, 2000, vol. 36, no. 5, pp. 932–941.
- Simon, R.D., Measurement of the cyanophycin granule polypeptide contained in the blue-green alga *Anabaena cylindrica*, *J. Bacteriol.*, 1973, vol. 114, no. 3, pp. 1213–1216.
- Solovchenko, A., Gorelova, O., Karpova, O., Selyakh, I., Semenova, L., Chivkunova, O., Baulina, O., Vinogradova, E., Pugacheva, T., Scherbakov, P., Vasilieva, S., Lukyanov, A., and Lobakova, E., Phosphorus feast and famine in cyanobacteria: is luxury uptake of the nutrient just a consequence of acclimation to its shortage?, *Cells*, 2020, vol. 9, no. 9, p. 1933.
- Stanier, R., Kunisawa, R., Mandel, M., and Cohen-Bazire, G., Purification and properties of unicellular blue-green algae (order Chroococcales), *Microbiol. Mol. Biol. Rev.*, 1971, vol. 35, no. 2, pp. 171–205.
- Stephan, D.P., Ruppel, H.G., and Pistorius, E.K., Interrelation between cyanophycin synthesis, L-arginine catabolism and photosynthesis in the cyanobacterium *Synechocystis* sp. strain PCC 6803, *Zeitschrift für Naturforschung C*, 2000, vol. 55, nos. 11–12, pp. 927–942.
- Stevens, S.E., Jr., Paone, D.A., and Balkwill, D.L., Accumulation of cyanophycin granules as a result of phosphate limitation in *Agmenellum quadruplicatum*, *Plant Physiol.*, 1981, vol. 67, no. 4, pp. 716–719.
- Stevens, S., Balkwill, D., and Paone, D., The effects of nitrogen limitation on the ultrastructure of the cyanobacterium *Agmenellum quadruplicatum*, *Arch. Microbiol.*, 1981, vol. 130, pp. 204–212.
- Su, Z., Oلمان, V., and Xu, Y., Computational prediction of Pho regulons in cyanobacteria, *BMC Genom.*, 2007, vol. 8, p. 156.
- Sun, X.-M., Ren, L.-J., Zhao, Q.-Y., Ji, X.-J., and Huang, H., Enhancement of lipid accumulation in microalgae by metabolic engineering, *Biochim. Biophys. Acta-Mol. Cell Biol. Lipids*, 2019, vol. 1864, no. 4, pp. 552–566.
- Teikari, J., Österholm, J., Kopf, M., Battchikova, N., Wahlsten, M., Aro, E.-M., Hess, W.R., and Sivonen, K., Transcriptomic and proteomic profiling of *Anabaena* sp. strain 90 under inorganic phosphorus stress, *Appl. Environ. Microbiol.*, 2015, vol. 81, no. 15, pp. 5212–5222.
- Tetu, S.G., Brahamsha, B., Johnson, D.A., Tai, V., Phillippy, K., Palenik, B., and Paulsen, I.T., Microarray analysis of phosphate regulation in the marine cyanobacterium *Synechococcus* sp. WH8102, *The ISME J.*, 2009, vol. 3, no. 7, pp. 835–849.
- Trentin, G., Piazza, F., Carletti, M., Zorin, B., Khozin-Goldberg, I., Bertuccio, A., and Sforza, E., Fixing N<sub>2</sub> into cyanophycin: continuous cultivation of *Nostoc* sp. PCC 7120, *Appl. Microbiol. Biotechnol.*, 2023, vol. 107, no. 1, pp. 97–110.
- Wanner, G., Henkelmann, G., Schmidt, A., and Köst, H.-P., Nitrogen and sulfur starvation of the cyanobacterium *Synechococcus* 6301 an ultrastructural, morphometrical, and biochemical comparison, *Zeitschrift für Naturforschung C*, 1986, vol. 41, nos. 7–8, pp. 741–750.
- Zlenko, D.V., Protasova, E.A., Tsoraev, G.V., Sluchanko, N.N., Cherepanov, D.A., Friedrich, T., Ge, B., Qin, S., Maksimov, E.G., and Rubin, A.B., Anti-stokes fluorescence of phycobilisome and its complex with the orange carotenoid protein, *Biochim. Biophys. Acta-Bioenergetics*, 2024, vol. 1865, no. 1, p. 149014.

**Publisher's Note.** Pleiades Publishing remains neutral with regard to jurisdictional claims in published maps and institutional affiliations. AI tools may have been used in the translation or editing of this article.